# Gold Nanorod–Photosensitizer Complex for Near-Infrared Fluorescence Imaging and Photodynamic/Photothermal Therapy *In Vivo*

**Boseung Jang,[†] Jin-Young Park,[†] Ching-Hsuan Tung,[‡] In-Hoo Kim,[†] and Yongdoo Choi[†,*]**

[†]Molecular Imaging & Therapy Branch, National Cancer Center, 111 Jungbalsan-ro, Ilsandong-gu, Goyang, Gyeonggi-do 410-769, South Korea, and [‡]Department of Radiology, The Methodist Hospital Research Institute, Weill Medical College of Cornell University, 6565 Fannin Street, #B5-022, Houston, Texas 77030, United States

**ABSTRACT** A gold nanorod (GNR)–photosensitizer complex was developed for noninvasive near-infrared fluorescence imaging and cancer therapy. We showed that (a) fluorescence emission and singlet oxygen generation by $AlPcS_4$ were quenched after complex formation with GNRs; (b) 4-fold greater intracellular uptake and better *in vitro* phototoxicity were observed in GNR–$AlPcS_4$-treated cells than in free $AlPcS_4$-treated cells; and (c) after intravenous injection of the GNR–$AlPcS_4$ complex, tumor sites were clearly identified on near-infrared fluorescence images as early as 1 h after injection. The tumor-to-background ratio increased over time and was 3.7 at 24 h; tumor growth reduced by 79% with photodynamic therapy (PDT) alone and by 95% with dual photothermal therapy (PTT) and PDT. This novel multifunctional nanomedicine may be useful for near-infrared fluorescence imaging and PTT/PDT in various cancers.

**KEYWORDS:** photodynamic therapy · gold nanorod · NIR fluorescence imaging · photothermal therapy · *in vivo*

In this study, we introduce a gold nanorod (GNR)–photosensitizer complex as a multifunctional nanomedicine platform for noninvasive *in vivo* near-infrared (NIR) fluorescence imaging and cancer therapy. Recently, GNRs have attracted attention for their interesting optical properties, including some which may have biomedical applications. First, GNRs produce a strong surface plasmon absorption band in the NIR region and may have utility as ultraefficient energy quenchers due to their immense absorption coefficients $10^4$-fold to $10^6$-fold higher than those of conventional organic dyes.[1,2] The peak absorption band in the NIR region can be easily tuned by adjusting its aspect size and ratio.[3] In addition, gold nanoparticles, including GNRs, can quench the excited energy of fluorochromes even at a distance of ~40 nm.[4] Second, poly(ethylene glycol)-conjugated GNRs are circulated in the blood for prolonged periods[5,6] and may serve as drug delivery carriers for passive targeting of cancers owing to their enhanced permeability and retention (EPR).[7] Third, the GNR itself can serve as a drug for hyperthermic treatment of cancers. Recent studies have shown that GNRs accumulated in tumor sites can produce heat and selectively ablate tumors by absorbing externally applied NIR light.[6,8]

Photodynamic therapy (PDT) is a promising treatment modality for cancers and other malignant diseases. Type II photosensitizers used in PDT are nontoxic to cells in the absence of light.[9] When exposed to light of an appropriate wavelength, these sensitizers become energized and begin to emit NIR fluorescence and generate reactive oxygen species including singlet oxygen. Owing to this action, tumors can be selectively destroyed using local illumination, while avoiding the severe side effects associated with conventional chemotherapy. However, the limited tumor selectivity of PDT agents has been the main drawback in the use of PDT because nonspecific activation of singlet oxygen generation from photosensitizers can be induced in normal tissues upon exposure to light.

Therefore, we hypothesized that fluorescence emission and singlet oxygen generation (SOG) by photosensitizers may be effectively controlled by manipulating the distance between the GNRs and photosensitizers (Figure 1). For example, when photosensitizers are located near a GNR surface, energy transfer from the photosensitizer to the GNR is effective, and the photosensitizers may become nonfluorescent and nonphototoxic. Thus, the GNR–photosensitizer

*Address correspondence to ydchoi@ncc.re.kr.

Received for review October 12, 2010 and accepted January 6, 2011.

**Published online January 18, 2011**
**10.1021/nn102722z**

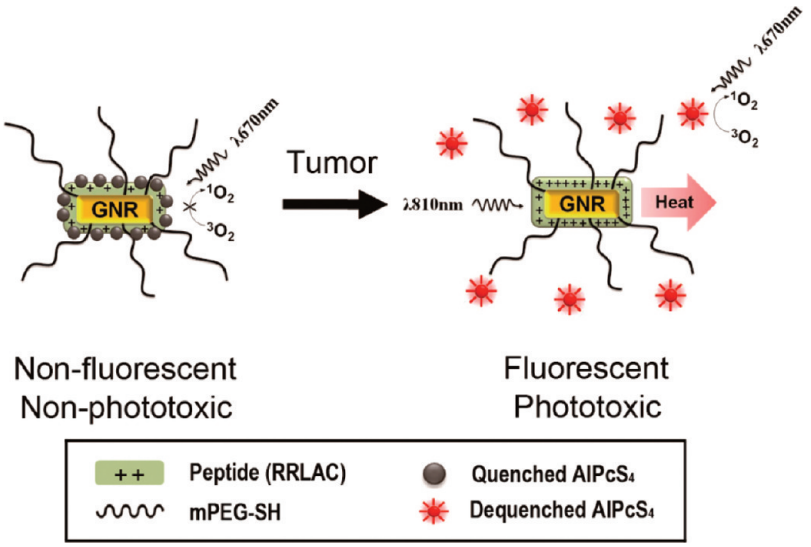


**Figure 1. Schematic diagram of the GNR−$AlPcS_4$ complex for NIR fluorescence imaging and tumor phototherapy.**

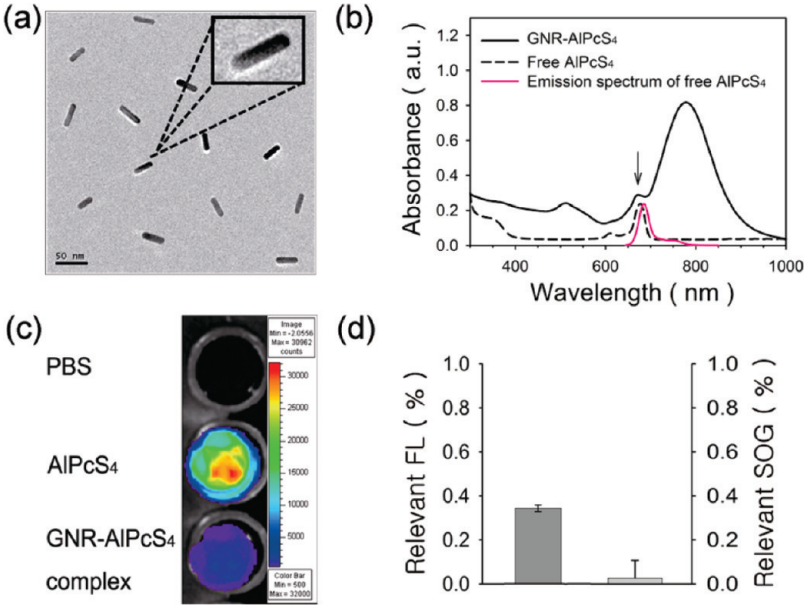


**Figure 2. (a) Transmission electron microscopy (TEM) image of GNRs. (b) Absorption spectra of the GNR−$AlPcS_4$ complex and free $AlPcS_4$; emission spectrum of free $AlPcS_4$. The arrow indicates the absorption peak of bound $AlPcS_4$ on the surface of GNRs. (c) NIR fluorescence images of PBS, free $AlPcS_4$, and the GNR−$AlPcS_4$ complex (final concn = 10 $\mu$M $AlPcS_4$ equiv) solution at the Cy5.5 channel. (d) Relevant fluorescence intensity (left) and SOG (right) of 10 $\mu$M of the GNR−$AlPcS_4$ complex. (The measured fluorescence and SOG of 10 $\mu$M $AlPcS_4$ was converted to 100%.)**

complex is nonfluorescent and nonphototoxic while in the circulatory system. A passive targeting mechanism localizes the complex in tumor tissue, where the photosensitizers are released from the GNR surface and become highly fluorescent and phototoxic. The tumor can then be detected by NIR fluorescence imaging with a high signal-to-background ratio. The tumor tissues visualized by NIR fluorescence can be selectively destroyed in a noninvasive manner by illumination of the detected tumors with NIR light during PDT while minimizing phototoxic tissue damage of the surrounding normal tissues. Therapeutic efficacy of GNR−photosensitizer complexes may be enhanced by additional photothermal therapy (PTT) with GNRs.

## RESULTS AND DISCUSSION

Cetyltrimethylammonium bromide (CTAB)-coated GNR was prepared by the seed-mediated method.[10] A TEM image of the CTAB-coated GNR showed that the average length and width were 33.7 ± 3.5 and 9.1 ± 1.4 nm, respectively (about 3.7:1 aspect ratio) (Figure 2a). Thiol-terminated monomethoxy poly(ethylene glycol) (mPEG-SH) and positively charged short peptide RRLAC were sequentially conjugated on the surface

of the GNR through thiol chemistry. Hydrophobic amino acids leucine (L) and alanine (A) were introduced to promote self-assembly of the peptides on the GNR surface. Positively charged arginine (R) was introduced to form a charge complex with the negatively charged photosensitizers (Supporting Information, Figure S1a). Conjugating mPEG-SH before RRLAC helps prevent aggregation of GNRs during the conjugation process. When RRLAC was conjugated first on the GNR surface before PEGylation, the GNR formed an aggregate during the RRLAC conjugation process (Supporting Information, Figure S1b). PEG−GNR−RRLAC prepared in this study showed a strong absorption band in the NIR region (Figure 2b). The zeta potentials of the CTAB-coated GNR, PEG−GNR, and PEG−GNR−RRLAC were +53.1, −4.34, and +37 mV, respectively. The negatively charged photosensitizer Al(III) phthalocyanine chloride tetrasulfonic acid ($AlPcS_4$) was then incorporated onto the positively charged PEG−GNR−RRLAC by mixing the $AlPcS_4$ and PEG−GNR−RRLAC aqueous solutions for 12 h to yield a PEG−GNR−RRLAC/$AlPcS_4$ charge complex (*i.e.*, a GNR−$AlPcS_4$ complex). After removal of the remaining free $AlPcS_4$, a new peak at 675 nm, corresponding to $AlPcS_4$, appeared. The zeta potential of the GNR−$AlPcS_4$ complex was measured as −8.44 mV, which indicated that $AlPcS_4$, a negative charge, was bound to the positively charged peptide by a charge−charge interaction, and thus the charge at the surface of the GNR was changed from positive to negative. From the UV/vis absorption spectrum, the molar ratio of bound $AlPcS_4$ per GNR was calculated at 2500:1.

The $AlPcS_4$ used in this study is a second-generation photosensitizer that has good optical properties for NIR fluorescence imaging and PDT. Its molar extinction coefficient, fluorescence quantum yield, and singlet oxygen quantum yield at about 675 nm are reported to be 170 000 $M^{-1}$ $cm^{-1}$, 0.59, and 0.38, respectively.[11−13] Since the main absorption band of the GNR in the NIR region significantly overlapped with the emission band of $AlPcS_4$ (Figure 2b), we assumed that fluorescence and also SOG of $AlPcS_4$ may be inhibited due to energy transfer from the excited $AlPcS_4$ to the GNR and also due to self-quenching between the bound photosensitizers. When the NIR fluorescence of PBS, $AlPcS_4$, and the GNR−$AlPcS_4$ complex solution was visualized with the fluorescence imaging system at the Cy5.5 channel (ex = 615−665 nm, em = 695−770 nm), fluorescence quenching was observed in the GNR−$AlPcS_4$ complex solution (Figure 2c). The fluorescence and SOG inhibitory characteristics of the GNR were quantified. The GNR−$AlPcS_4$ complex had a fluorescence intensity corresponding to 0.4% and a SOG efficiency of 0.03% based on free $AlPcS_4$ (Figure 2d). This confirms that, when $AlPcS_4$ is adjacent to the GNR surface, the fluorescent signal and SOG are effectively inhibited. In other words, the fluorescence and SOG of $AlPcS_4$ recover when the compound is released from the GNR surface. About 80% of the bound $AlPcS_4$ is released slowly over 24 h in a physiological buffer solution (Supporting Information, Figure S2).

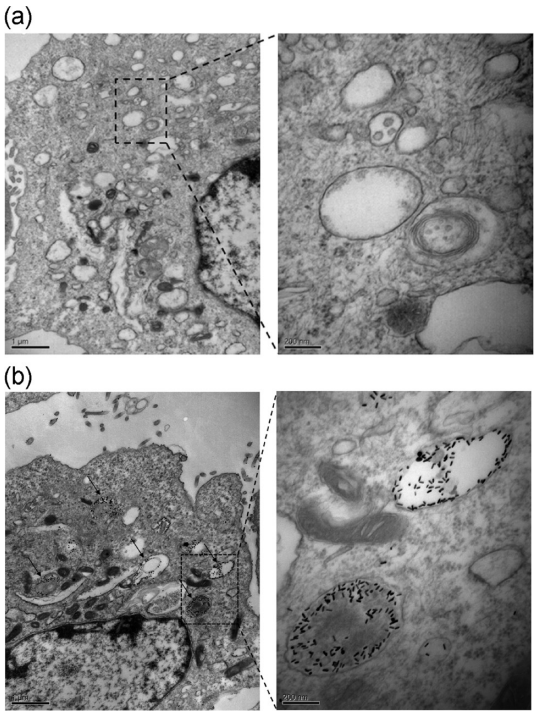


**Figure 3. TEM images of SCC7 cells treated with (a) free $AlPcS_4$ and (b) the GNR−$AlPcS_4$ complex. In the case of the GNR−$AlPcS_4$ complex-treated cells, many GNRs are seen in the cytosolic vesicles. The arrows indicate cytosolic vesicles containing GNRs.**

Dispersion stability of the GNR−$AlPcS_4$ complex in the presence of serum proteins was tested prior to the *in vitro* cell studies. For comparison, the CTAB-coated GNR and the GNR−$AlPcS_4$ complex were dispersed in each of the following: deionized water, phosphate buffered saline (PBS), and cell culture media containing 10% fetal bovine serum (FBS). The GNR−$AlPcS_4$ complex was well-dispersed in all test solutions and showed no aggregation behavior for 7 days (Supporting Information, Figure S3). Although CTAB-coated GNRs were shown to be stable in both deionized water and PBS, they formed aggregates in the cell culture media containing FBS and sedimented out of solution within 4 h. This indicates that PEGs on the surface of the GNR−$AlPcS_4$ complex were enough to prevent interaction between serum proteins and GNRs, which is important to achieve a long blood half-life of GNRs *in vivo*.

Squamous cell carcinoma (SCC7) cells were treated with free $AlPcS_4$ and the GNR−$AlPcS_4$ complex to evaluate the degree of photosensitizer uptake into the cancer cells. When a cross section of photosensitizer-treated cells was observed by TEM, GNRs were easily seen inside the GNR−$AlPcS_4$ complex-treated SCC7 cells, and many of them were in the cytosolic vesicles, such as the endosomes and lysosomes (Figure 3); the GNR−$AlPcS_4$ complex was therefore

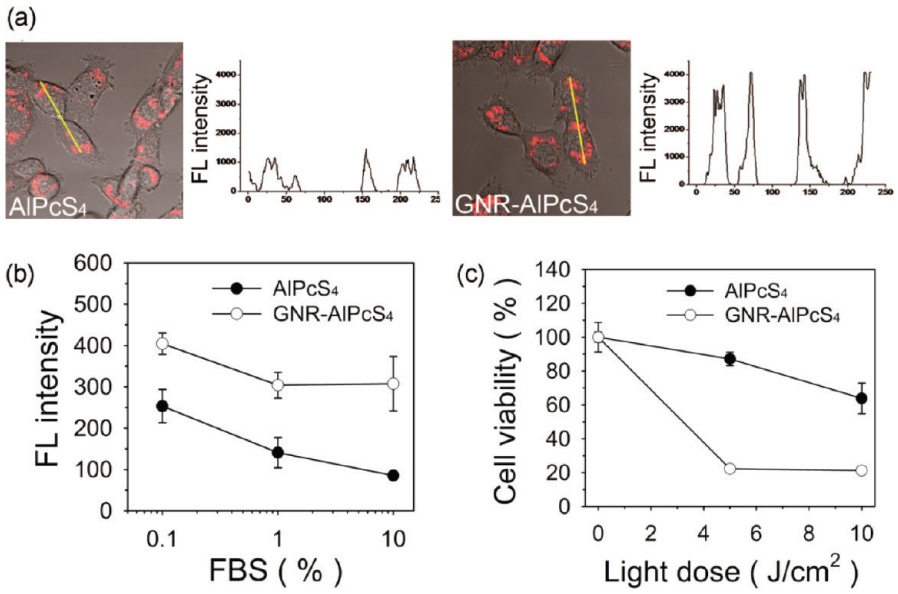


**Figure 4. Intracellular uptake and *in vitro* phototoxicity of the GNR−$AlPcS_4$ complex. (a) Confocal microscopy images of SCC7 cells incubated for 4 h in free $AlPcS_4$ and the GNR−$AlPcS_4$ complex (5 $\mu$M $AlPcS_4$ equiv). Left picture: fluorescence image (red color indicates fluorescence signals from $AlPcS_4$). Right graph: fluorescence intensity analyzed from the yellow line on the left images. (b) Effect of serum concentration on the intracellular uptake of free $AlPcS_4$ and the GNR−$AlPcS_4$ complex ($n$ = 4). (c) *In vitro* phototoxicity of free $AlPcS_4$ and the GNR−$AlPcS_4$ complex (final concn = 5 $\mu$M $AlPcS_4$ eq, $n$ = 4).**

internalized *via* the endocytic pathway. About 4-fold greater fluorescence was detected in the GNR−$AlPcS_4$ complex-treated cells than in the free $AlPcS_4$-treated cells (confocal micrographs, Figure 4a), which means cellular uptake of $AlPcS_4$ was greatly improved by complexing with GNR. Cellular uptake of photosensitizers is significantly reduced in serum because nonspecific binding to serum proteins prevents intracellular uptake of many photosensitizers.[14,15] $AlPcS_4$ is also known to bind serum albumin with high affinity, predominantly by electrostatic interaction.[16] We studied the effect of serum proteins on the intracellular uptake of $AlPcS_4$ by measuring the amount of $AlPcS_4$ taken up into SCC7 cells in the presence of different serum concentrations in the cell culture media. Fluorescence intensities of $AlPcS_4$ from cell lysates were measured and compared. As shown in Figure 4b, cellular uptake of free $AlPcS_4$ significantly decreased with increasing serum concentrations, indicating that reduced $AlPcS_4$ uptake is due to the nonspecific binding of the photosensitizer molecules to serum proteins. In contrast, cellular uptake of GNR-complexed $AlPcS_4$ was not much affected by serum concentration, resulting in much better internalization in the cancer cells. Because cytotoxic singlet oxygen has a very short radius of action (<0.02 $\mu$m) in comparison with the size of tumor cells (≥10 $\mu$m),[17] cellular internalization of photosensitizers is important for inducing photodynamic damage to cancer cells.[18] In other words, photosensitizers in the extracellular space do not effectively damage cancer cells even if they are accumulated within tumor tissue. Complexing $AlPcS_4$ to PEGylated GNRs improves intracellular uptake of $AlPcS_4$ by about 4-fold. Therefore, GNR−$AlPcS_4$ complex phototoxicity was expected to be greater than that of free $AlPcS_4$ in *in vitro* and *in vivo* studies.

The phototoxicity of free $AlPcS_4$ and the GNR−$AlPcS_4$ complex was evaluated *in vitro* (Figure 4c). SCC7 cells treated with free $AlPcS_4$ exhibited reduced cell viability with increasing light dose, and 36% of the SCC7 cells were dead at a light dose of 10 J $cm^{-2}$. When the cells were treated with the GNR−$AlPcS_4$ complex (4 h after incubation, 5 $\mu$M $AlPcS_4$ equiv), 78% of the SCC7 cells were dead at a light dose of 5 J $cm^{-2}$. Dark toxicity was observed in neither the free $AlPcS_4$ nor the GNR−$AlPcS_4$ complex-treated cells.

We used a xenografted mouse tumor model to assess the utility of the GNR−$AlPcS_4$ complex for *in vivo* cancer imaging. The SCC7 cell line was subcutaneously implanted into the hind flank of each mouse, and the tumor was allowed to grow to about 20 $mm^3$. Following intravenous injection with PBS (4 mice, 150 $\mu$L/mouse), free $AlPcS_4$ (3 mice, 1 mg $AlPcS_4$ equiv $kg^{-1}$), and the GNR−$AlPcS_4$ complex (5 mice, 1 mg $AlPcS_4$ equiv $kg^{-1}$), NIR fluorescence images (Cy5.5 channel) were obtained 1, 4, and 24 h after injection, respectively (Figure 5a). In the mice receiving both free $AlPcS_4$ and the GNR−$AlPcS_4$ complex, tumor sites showed higher fluorescence intensities from the initial imaging time point, indicating greater accumulation of the injected photosensitizers in the tumor sites. In particular, tumor sites in the GNR−$AlPcS_4$ complex group were clearly discriminated from the surrounding normal tissues 1 h after injection. As shown in the fluorescence images, background signals produced from the tumor's surroundings were much lower

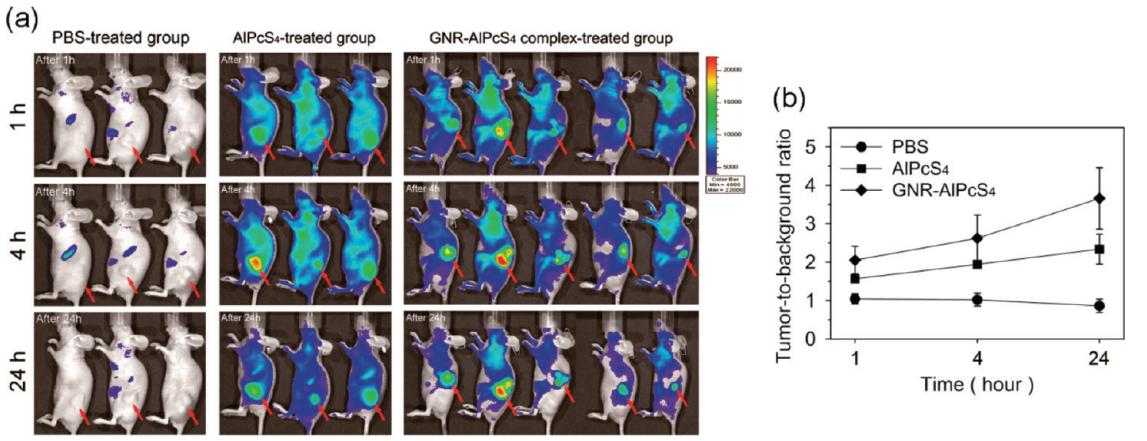


**Figure 5. Evaluation of NIR fluorescence images *in vivo*. (a) Near-infrared (NIR) fluorescence images (Cy5.5 channel) of PBS (left), free $AlPcS_4$-treated (middle), and GNR−$AlPcS_4$ complex-treated (right) mice were obtained 1, 4, and 24 h after injection. The arrows indicate tumor sites. (b) Tumor-to-background ratio (TBR) calculated from the NIR fluorescence images at 1, 4, and 24 h. Symbols indicate the PBS-treated group ($n$ = 4), the free $AlPcS_4$-treated group ($n$ = 3), and the GNR−$AlPcS_4$ complex-treated group ($n$ = 5).**

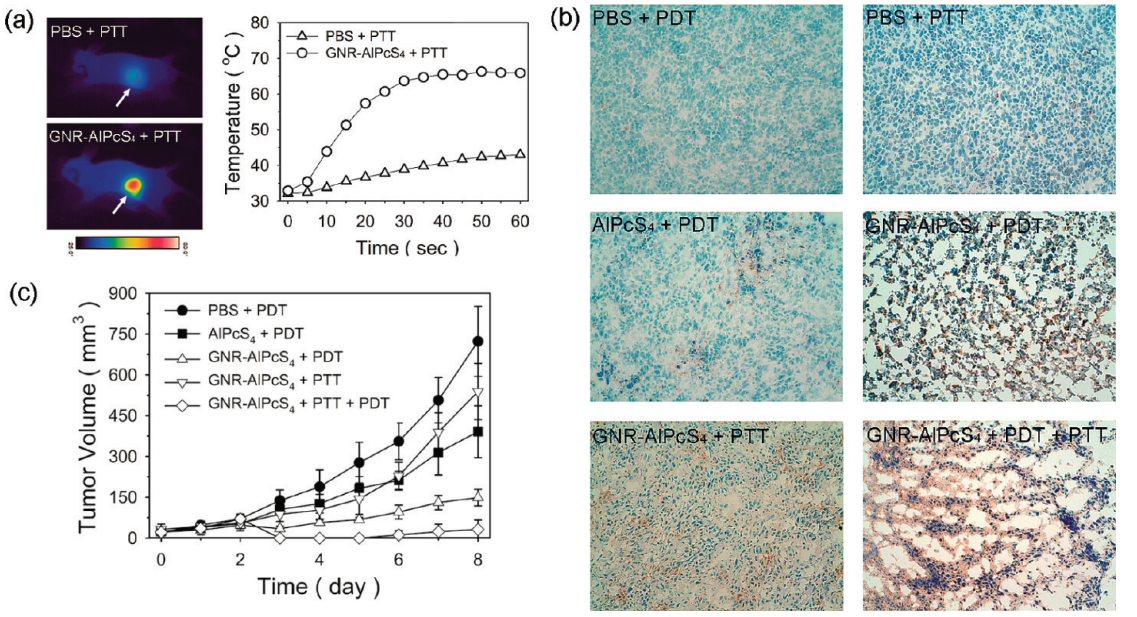


**Figure 6. *In vivo* PDT and PTT. (a) Thermographic images captured after 1 min of light illumination, and thermographic monitoring in the tumors of GNR−$AlPcS_4$-injected and PBS-injected mice. (b) TUNEL staining of the tissue sections (magnification ×20). Normal or apoptotic cell nuclei are shown in green and brown, respectively. Empty areas in the tissue sections (GNR−$AlPcS_4$ complex + PDT and GNR−$AlPcS_4$ complex + PTT + PDT) are due to washout of the destroyed tumor cells during the staining procedure. (c) Tumor size after each therapy session. Points, mean; bars, standard deviation; PBS + PDT ($n$ = 7); free $AlPcS_4$ + PDT ($n$ = 7); GNR−$AlPcS_4$ complex + PDT ($n$ = 7); GNR−$AlPcS_4$ complex + PTT ($n$ = 5); GNR−$AlPcS_4$ complex + PTT + PDT ($n$ = 7); $n$ = number of tumors involved.**

in the GNR−$AlPcS_4$ complex group. The tumor-to-background ratio (TBR) of fluorescence increased with time (Figure 5b) and reached a maximum 24 h after injection. The mean TBR values at 24 h were 3.7 for GNR−$AlPcS_4$ complex-treated mice and 2.3 for free $AlPcS_4$-treated mice.

Although the GNR−$AlPcS_4$ complex was expected to enhance delivery of $AlPcS_4$ to tumor sites, similar fluorescence intensities at the tumor site were noted 24 h after injection in mice treated with free $AlPcS_4$ and in those treated with GNR−$AlPcS_4$. We hypothesize that some amount of $AlPcS_4$ in tumor tissues was still located on or near the GNR surface, and therefore, its fluorescence was quenched and could not be detected by NIR fluorescence imaging. Therefore, we assumed that the bound photosensitizers might be detached from the GNR surface by heating, resulting in the recovery of the quenched fluorescence. A recent study by Kuo *et al.* also demonstrated stimulated drug release from the GNR surface by heat generation during NIR light illumination.[19] To verify this assumption, free $AlPcS_4$ and the GNR−$AlPcS_4$ complex were intravenously injected into five tumor-bearing mice. The tumor sites were irradiated with an 810 nm CW

laser (3.82 W $cm^{-2}$, 229 J $cm^{-2}$) 24 h after injection. Upon illumination, tumor surface temperatures reached about 65 °C (Figure 6a) and fluorescence intensity increased by 1.5-fold (Supporting Information, Figure S4), indicating that hyperthermia released the bound photosensitizers, which then regained their fluorescence and photosensitivity. No change (*i.e.*, 1.07 ± 0.05 times) in fluorescence intensity was observed before and after illumination of the free $AlPcS_4$-treated mice. Therefore, it seems at least 1.5-fold more $AlPcS_4$ accumulated in tumors when $AlPcS_4$ was delivered in complex with GNR.

*In vivo* therapeutic efficacy was first investigated by thermographic analyses of tumor hyperthermia during NIR illumination. As shown in Figure 6a, the maximum temperature of the tumor surface in the PBS-treated mouse was only about 43 °C during PTT (810 nm, 3.82 W $cm^{-2}$, 229 J $cm^{-2}$). In contrast, tumor temperature in the GNR−$AlPcS_4$ complex-treated mouse rapidly reached ablative temperatures of >60 °C within 25 s of 810 nm illumination and was maintained at about 65 °C thereafter. Temperatures above 60 °C cause instantaneous coagulative necrosis and irreversible cell death.[20] Tumor temperature in the GNR−$AlPcS_4$ complex-treated mouse did not increase upon 670 nm illumination (331 mW $cm^{-2}$, 60 J $cm^{-2}$), indicating that no hyperthermic effect was induced by PDT irradiation conditions (data not shown here). One day after light treatment, tumor tissues were collected from the mice and tumor sections were stained using the TUNEL technique with the ApopTag kit to assess tissue damage. As shown in Figure 6b, tumor sections from PBS-treated mice showed no signs of tissue damage after either PDT or PTT. Stained tumors sections from $AlPcS_4$-treated mice showed an increased number of brown spots, indicating that some apoptotic damage was induced after PDT. In mice injected with GNR−$AlPcS_4$ and irradiated with NIR lights (*i.e.*, either 670 nm alone or 810 nm/670 nm combined), TUNEL staining clearly showed severe apoptosis and significant tissue loss across a large tumor area. Interestingly, polymorphonuclear (PMN) cells were rarely, if ever, seen in the tumors that received dual PTT/PDT therapy, although many PMN cells were observed in the tumors treated with PDT alone. In mice injected with GNR−$AlPcS_4$ and treated with PTT alone, tumor apoptosis was increased somewhat beyond that in the $AlPcS_4$-treated mice but not as significant as in mice treated with PDT alone or PTT/PDT dual therapy.

The anticancer efficacy of GNR−$AlPcS_4$ was further evaluated by measuring tumor growth rates. When their tumor sizes reached about 20 $mm^3$ (day 0), the 33 mice were divided into 5 groups. Mice in groups 1 and 2 received an intravenous injection of either sterilized PBS (150 $\mu$L/mouse) or free $AlPcS_4$ solution (1 mg $AlPcS_4$ $kg^{-1}$) on day 1, followed by PDT light treatment (670 nm, 331 mW $cm^{-2}$, 60 J $cm^{-2}$) 24 h after injection (day 2). Mice in groups 3, 4, and 5 received an intravenous injection of GNR−$AlPcS_4$ solution (1 mg $AlPcS_4$ equiv $kg^{-1}$) on day 1. After injection (24 h), mice in group 3 were irradiated with a 670 nm CW laser for PDT (331 mW $cm^{-2}$, 60 J $cm^{-2}$). Mice in group 4 received PTT (810 nm, 3.82 W $cm^{-2}$, 229 J $cm^{-2}$). Mice in group 5 received PTT first, followed by PDT. Remarkably, enhanced *in vivo* therapeutic effects were observed in the GNR−$AlPcS_4$ complex-treated groups compared with that in the free $AlPcS_4$-treated group (Figure 6c). The mean tumor sizes in groups 3 and 5 were 20.6% ($P < 0.001$) and 5.1% ($P < 0.001$), respectively, on day 8 compared with group 1. No apparent tumor mass was detected for any of the 7 mice in group 5 until day 5, and a tiny tumor mass was detected in 3 mice on day 8 (Supporting Information, Figure S5). On day 13, no detectable tumor mass was seen in 3 of the 7 mice. The PTT-only treated mice in group 4 also showed slightly improved therapeutic outcomes in comparison to group 2 on days 3−5, which corresponds with the TUNEL staining results. However, tumor growth rate was reversed after day 6 due to rapid regrowth of the surviving cancer cells. Although a remarkable therapeutic effect was not obtained with PTT in comparison to PDT in this study, optimization of the PTT irradiation conditions may enhance the therapeutic outcome of treatment with GNR−$AlPcS_4$ for tumor hyperthermia.

## CONCLUSION

We have verified that the GNR−$AlPcS_4$ complex is not only useful for NIR fluorescence imaging of tumor sites but also helpful for improving therapeutic efficacy *in vivo*. By combining $AlPcS_4$ with the GNR, highly effective PTT/PDT dual therapy becomes possible, although PDT alone was also proven effective for obtaining significant anticancer therapeutic effects. We are currently attempting the introduction of targeting ligands at the end of the PEG chain, which may further improve tumor targeting efficiency of GNR−photosensitizer complexes. We believe that the proposed GNR−photosensitizer complex may be used to visualize and treat various diseases that occur within reach of an endoscope.

## METHODS

**Preparation of GNRs.** GNRs were prepared by a seed-mediated method as described by Hongwei *et al.*[10] In brief, the method was as follows: the seed solution was prepared by mixing cetyltrimethylammonium bromide (CTAB) solution (7.5 mL, 100 mM CTAB in deionized water) with 250 $\mu$L of 10 mM $HAuCl_4$

aqueous solution. While the mixture was stirred at 400 rpm, 600 $\mu$L of 10 mM $NaBH_4$ was added, and the mixture was stirred at 900 rpm for 2 min; subsequently, it was maintained at 25 °C for 2 h. Meanwhile, 1.7 mL of 10 mM $HAuCl_4$ aqueous solution was added to 40 mL of 100 mM CTAB aqueous solution, followed by sequential addition of 250 $\mu$L of 10 mM $AgNO_3$ aqueous solution and 270 $\mu$L of 100 mM ascorbic acid aqueous solution. Thereafter, 420 $\mu$L of the seed solution was added and reacted for 12 h; the reaction mixture was then centrifuged at 15 000*g* at 25 °C for 15 min to obtain the GNRs.

**Preparation of PEG−GNR−RRLAC.** Aqueous solution containing CTAB-coated GNRs were centrifuged at 15 000*g* for 15 min and decanted; the GNRs were then resuspended in deionized water to remove excess CTAB. The concentration of GNR solution was 150 nM after resuspension. To conjugate monomethoxy poly(ethylene glycol) thiol (mPEG-SH; MW 5000 kDa; SunBio, Inc.), 100 $\mu$L of mPEG-SH (1 mM) solution was added to 500 $\mu$L of 150 nM GNR solution and stirred at 25 °C for 20 h. The GNR solution was then centrifuged, decanted, and redispersed in deionized water three times to remove unreacted mPEG-SH. Finally, 900 $\mu$L of PEGylated GNR (PEG−GNR) aqueous solution was obtained. The RRLAC peptide (MW 617.34 Da, Peptron Inc.) was dissolved in deionized water to prepare a 2 mM RRLAC peptide solution. The RRLAC solution (100 $\mu$L, 2 mM peptide) was added to 900 $\mu$L of the PEG−GNR solution and stirred at 25 °C for 12 h to further conjugate the peptides on the PEG−GNR surface. The mixture was centrifuged, decanted, and redispersed in deionized water three times to remove unconjugated peptides. The GNRs were finally redispersed in 500 $\mu$L of deionized water to obtain the PEG−GNR−RRLAC solution in which both the PEG and RRLAC peptides were conjugated on the GNR surface. Both mPEG-SH and RRLAC were conjugated on the surface of GNR through a thiol chemistry. The number of conjugated RRLAC per GNR was calculated by analyzing the amount of unconjugated peptides in the supernatant by using high-performance liquid chromatography (HPLC), and the molar ratio was found to be 2667:1. HPLC analysis was performed on a Waters 2690 (Waters, USA) HPLC system equipped with XTerra RP18, 5 $\mu$m, 4.6 × 250 mm reverse-phase column. The mobile phase for HPLC analyses was acetonitrile (0.1% trifluoroacetic acid) with a flow rate of 1 mL/min at room temperature.

For comparison, PEG−GNR−RRLAC preparation was also attempted by changing the order of the conjugation procedure (*i.e.*, conjugating RRLAC first and then mPEG-SH). The overall conditions for conjugation, such as concentration of reagents and reaction time, were exactly the same, except that the order of conjugation of mPEG-SH and RRLAC was reversed. After completion of all the conjugation procedures, the UV/vis spectrum and zeta potential of the GNRs prepared were analyzed.

**Preparation of the GNR−$AlPcS_4$ Complex.** The GNR−photosensitizer charge complex was prepared by mixing the positively charged PEG−GNR−RRLAC with the negatively charged photosensitizer Al(III) phthalocyanine chloride tetrasulfonic acid ($AlPcS_4$, Frontier Scientific, Inc.). First, $AlPcS_4$ aqueous solution (100 $\mu$L, 4 mM) was added to 500 $\mu$L of the 150 nM PEG−GNR−RRLAC solution, and the mixture was stirred at 25 °C for 12 h to form a charge complex. Free $AlPcS_4$ that did not form a complex with PEG−GNR−RRLAC was removed by passing the resulting solution through a PD-10 desalting column (GE Healthcare), thereby yielding a purified PEG−GNR−RRLAC/$AlPcS_4$ charge complex. To calculate the amounts of $AlPcS_4$ attached per GNR, the absorption spectrum of the purified GNR−$AlPcS_4$ complex solution was measured using a UV/vis scanning spectrophotometer (DU730, Beckman) immediately after the purification process. The CTAB-coated GNR has molar absorption coefficients of $1.3 \times 10^9$ and $4.6 \times 10^9$ $M^{-1}$ $cm^{-1}$ at 510 and 785 nm, respectively.[21] $AlPcS_4$ is known to have a molar absorption coefficient of $1.7 \times 10^5$ $M^{-1}$ $cm^{-1}$ at 675 nm.[11] These values were used to calculate the average number of $AlPcS_4$ bound per GNR in the GNR−$AlPcS_4$ complex.

**Analysis of Fluorescence and SOG from the GNR−$AlPcS_4$ Complex.** To observe fluorescence inhibitory characteristics, the GNR−$AlPcS_4$ complex and $AlPcS_4$ were dissolved in PBS (6.7 mM, pH 7.4, NaCl 154 mM), and their fluorescence values were measured (ex = 660 nm, em = 690 nm). In this study, 10 $\mu$M $AlPcS_4$ equiv was added in each solution. A fluorescence image of the 96-well plate containing PBS, $AlPcS_4$, and the GNR−$AlPcS_4$ complex aqueous solution was obtained using IVIS Lumina (Caliper Life Sciences, Cy5.5 channel: ex = 615−665 nm, em = 695−770 nm). To observe an inhibitory characteristic with respect to SOG, each of the $AlPcS_4$ and GNR−$AlPcS_4$ complex and a singlet-oxygen-detecting reagent (singlet oxygen sensor green, Molecular Probes) were dissolved in PBS (saturated with oxygen gas) solution containing $AlPcS_4$ and the GNR−$AlPcS_4$ complex. Each solution was irradiated with a CW laser bean at 670 nm (irradiation dose rate = 26.3 mW $cm^{-2}$, irradiation dose = 0.79 J $cm^{-2}$). SOG from the GNR−$AlPcS_4$ complex was quantified by comparing to that from free $AlPcS_4$. All experiments were performed in triplicate.

**Cellular Uptake of $AlPcS_4$ and the GNR−$AlPcS_4$ Complex TEM Analysis.** To examine cellular internalization of GNRs, we performed TEM investigation of the cancer cells treated with $AlPcS_4$ and the GNR−$AlPcS_4$ complex. Squamous cell carcinoma (SCC7) cells obtained from the American Type Culture Collection (Rockville, MD) were maintained in RPMI 1640 medium supplemented with 10% FBS (GIBCO, Invitrogen) and 1% penicillin−streptomycin (GIBCO, Invitrogen) in a humidified 5% $CO_2$ incubator at 37 °C. The SCC7 cells were dispensed into a 100 mm dish at a concentration of $5 \times 10^4$ cells/mL and incubated for 24 h for cell attachment. The free $AlPcS_4$ and $AlPcS_4$−GNR complex solution were added to the dishes at a concentration of 5 $\mu$M $AlPcS_4$ equiv. After 4 h of incubation, the cells were washed three times, trypsinized, centrifuged, and fixed. After further processing of the cells, sample sections were observed by TEM.

**Fluorescence Analysis.** The SCC7 cells were plated at a density of 90 000 cells/well onto a LabTek II chambered coverglass (Nalge Nunc International Corp.) and incubated for 24 h for cell attachment. The free $AlPcS_4$ and the GNR−$AlPcS_4$ complex were each dissolved in fresh RPMI medium with 10% FBS to achieve an equivalent concentration of 5 $\mu$M $AlPcS_4$. The existing cell culture medium was replaced with 600 $\mu$L of fresh medium containing $AlPcS_4$ or the GNR−$AlPcS_4$ complex. After the cells were incubated for 4 h, they were washed three times and a fresh cell culture medium was used. Subsequently, NIR fluorescence images (ex = 633 nm, em = 636−721 nm) were acquired using a confocal laser scanning microscope (ZEISS LSM 510 META). Fluorescence intensity from the cells was also analyzed using Axio vision software.

We further investigated the effect of serum concentration in the culture medium on the cellular uptake of the photosensitizers. SCC7 cells were seeded in each well of 96-well plates (9000 cells/well) and incubated for 24 h for cell attachment. Thereafter, fresh cell culture medium containing different percentages of FBS was used to dissolve free $AlPcS_4$ and the GNR−$AlPcS_4$ complex. After the existing culture medium was replaced with 200 $\mu$L of fresh medium containing free $AlPcS_4$ or the GNR−$AlPcS_4$ complex (5 $\mu$M $AlPcS_4$ equiv), the cells were incubated for 4 h. Subsequently, the cells were washed three times with PBS buffer and treated with 200 $\mu$L of 0.1% SDS/0.1 M NaOH solution for 2 h for cell lysis. Fluorescence signals from the cell lysates were measured using a fluorescence plate reader (ex = 660 nm, em = 690 nm).

***In Vitro* Phototoxicity Test.** SCC7 cells were seeded in each well of 96-well plates at a density of 9000 cells/well and incubated for 24 h. Thereafter, the $AlPcS_4$ and the GNR−$AlPcS_4$ complex were diluted with a cell culture medium containing 10% FBS to obtain an equivalent concentration of 5 $\mu$M $AlPcS_4$. The existing culture medium was replaced with 200 $\mu$L of fresh medium containing free $AlPcS_4$ or the GNR−$AlPcS_4$ complex, and the cells were incubated for 4 h. For the untreated control group, the same volume of fresh culture medium without photosensitizers was added to the plate. After the cells were washed twice, a fresh cell culture medium was added. The PDT-treated groups were irradiated with a 670 nm CW laser beam at doses of 5 and 10 J $cm^{-2}$ and at a dose rate of 50 mW $cm^{-2}$. The cells were incubated for an additional 24 h, and cell viability was measured using a cell counting kit-8 (Dojindo Laboratories). Cell viability was calculated as a percentage compared to untreated control cells. Dark toxicity of the free $AlPcS_4$ and GNR−$AlPcS_4$ complex was also evaluated by incubating these compounds for 4 h at the same concentration without light treatment.

***In Vivo* Studies in a Xenograft Tumor Model.** All animal studies were approved by the Institutional Animal Care and Use Committee. Female athymic nude mice (Balb/c-nu, *ca.* 19−22 g) were used for the *in vivo* experiments. SCC7 cells ($2 \times 10^6$ cells/0.05 mL of RPMI) were implanted subcutaneously into the hind flank of each mouse, and the tumor size was measured daily.[22] The animals were chosen for *in vivo* studies when their tumor sizes reached ~20 $mm^3$.

For *in vivo* NIR fluorescence imaging, three mice in the $AlPcS_4$-treated group and five mice in the GNR−$AlPcS_4$ complex-treated group received intravenous injections of the drug solution at a dose of 1 mg $AlPcS_4$ equiv/kg. Four mice in the control group received intravenous injections of sterilized PBS solution (150 $\mu$L/mouse). Drug solutions were prepared by dissolving $AlPcS_4$ and the GNR−$AlPcS_4$ complex in sterilized PBS (6.7 mM, pH 7.4, NaCl 154 mM). NIR fluorescence images were obtained using an IVIS Lumina (Cy5.5 channel, ex = 615−665 nm, em = 695−770 nm) at 1, 4, and 24 h after injection.

The effect of PTT on photosensitizer release from the GNR−$AlPcS_4$ complex was also investigated with the fluorescence imaging system. Five tumor-bearing mice received an intravenous injection of free $AlPcS_4$ (3 mice, 1 mg of $AlPcS_4$/kg) and GNR−$AlPcS_4$ complex (2 mice, 1 mg of $AlPcS_4$ equiv/kg). Twenty-four hours after drug injection, NIR fluorescence images were obtained before and immediately following PTT (irradiation condition = 810 nm, 3.82 W $cm^{-2}$, 229 J $cm^{-2}$).

To investigate tumor hyperthermia and tissue damage upon light illumination, 12 mice were tested. Briefly, four mice in the control group received intravenous injection with sterilized PBS solution, followed by light treatment using a 670 nm CW laser for PDT (2 mice, 331 mW $cm^{-2}$, 60 J $cm^{-2}$) and an 810 nm CW laser for PTT (2 mice, 3.82 W $cm^{-2}$, 229 J $cm^{-2}$) 24 h after injection. Two mice in the $AlPcS_4$-treated group received intravenous injection of the free $AlPcS_4$ solution (1 mg of $AlPcS_4$/kg) followed by light treatment for PDT 24 h after injection. Six mice in the GNR−$AlPcS_4$ complex-treated group received intravenous injection of the GNR−$AlPcS_4$ complex solution (1 mg of $AlPcS_4$ equiv/kg) followed by light treatment using a 670 nm CW laser for PDT (2 mice), an 810 nm CW laser for PTT (2 mice), and sequential PTT/PDT dual therapy (2 mice) 24 h after injection. Increasing temperatures in tumor tissues during PDT and PTT were measured by using an IR camera to record thermal images of PBS-treated mice and GNR−$AlPcS_4$ complex-treated mice (FLIR, Thermovision A40) in real time during 670 and 810 nm light illumination. The temperature increase was analyzed using ThermaCAM Researcher software. One day after light treatment, tumor tissues from all mice were collected, dipped into OCT compound, sectioned, and stained using the TUNEL technique with the ApopTag kit (Chemicon). Normal or apoptotic nuclei were stained green and brown, respectively.

For the *in vivo* tumor growth study, 33 mice were divided into 5 groups on day 0. Mice in groups 1 and 2 received intravenous injections of either sterilized PBS (7 mice, 150 $\mu$L/mouse) or free $AlPcS_4$ solution (7 mice, 1 mg of $AlPcS_4$/kg) on day 1, followed by light treatment for PDT (670 nm, 331 mW $cm^{-2}$, 60 J $cm^{-2}$) 24 h after injection (day 2). Mice in groups 3, 4, and 5 received intravenous injection of the GNR−$AlPcS_4$ complex solution (1 mg of $AlPcS_4$ equiv/kg) on day 1. After 24 h, mice in group 3 were irradiated with a 670 nm CW laser beam for PDT (7 mice, 331 mW $cm^{-2}$, 60 J $cm^{-2}$). Mice in group 4 received PTT (5 mice, 810 nm, 3.82 W $cm^{-2}$, 229 J $cm^{-2}$). Mice in group 5 received PTT first (7 mice, 810 nm, 3.82 W $cm^{-2}$, 229 J $cm^{-2}$) and then PDT (670 nm, 331 mW $cm^{-2}$, 60 J $cm^{-2}$). Thereafter, tumor volumes were measured daily. When the tumor sizes of the control group exceeded 700 $mm^3$ (day 8), the measurements were halted in all groups, except group 5, which was monitored until day 13.

**Statistical Analysis.** Data are expressed as mean ± standard deviation. Student's *t*-test was used for statistical analyses.

*Acknowledgment.* This work was supported by a grant (0710680 and 0931470) from National Cancer Center, the Fundamental R&D Program for Core Technology of Materials by the Ministry of Knowledge Economy, and the Pioneer Research Center Program through the National Research Foundation of Korea funded by the Ministry of Education, Science and Technology (2010-0002209), Republic of Korea.

*Supporting Information Available:* Additional experimental details. This material is available free of charge *via* the Internet at http://pubs.acs.org.

## REFERENCES AND NOTES

1. Dulkeith, E.; Ringler, M.; Klar, T. A.; Feldmann, J.; Munoz Javier, A.; Parak, W. J. Gold Nanoparticles Quench Fluorescence by Phase Induced Radiative Rate Suppression. *Nano Lett.* **2005,** *5*, 585–589.
2. Jain, P. K.; Lee, K. S.; El-Sayed, I. H.; El-Sayed, M. A. Calculated Absorption and Scattering Properties of Gold Nanoparticles of Different Size, Shape, and Composition: Applications in Biological Imaging and Biomedicine. *J. Phys. Chem. B* **2006,** *110*, 7238–7248.
3. Nikoobakht, B.; El-Sayed, M. A. Preparation and Growth Mechanism of Gold Nanorods (NRs) Using Seed-Mediated Growth Method. *Chem. Mater.* **2003,** *15*, 1957–1962.
4. Griffin, J.; Singh, A. K.; Senapati, D.; Rhodes, P.; Mitchell, K.; Robinson, B.; Yu, E.; Ray, P. C. Size- and Distance-Dependent Nanoparticle Surface-Energy Transfer (NSET) Method for Selective Sensing of Hepatitis C Virus RNA. *Chemistry* **2009,** *15*, 342–351.
5. Niidome, T.; Yamagata, M.; Okamoto, Y.; Akiyama, Y.; Takahashi, H.; Kawano, T.; Katayama, Y.; Niidome, Y. PEG-Modified Gold Nanorods with a Stealth Character for *In Vivo* Applications. *J. Controlled Release* **2006,** *114*, 343–347.
6. von Maltzahn, G.; Park, J. H.; Agrawal, A.; Bandaru, N. K.; Das, S. K.; Sailor, M. J.; Bhatia, S. N. Computationally Guided Photothermal Tumor Therapy Using Long-Circulating Gold Nanorod Antennas. *Cancer Res.* **2009,** *69*, 3892–3900.
7. Hashizume, H.; Baluk, P.; Morikawa, S.; McLean, J. W.; Thurston, G.; Roberge, S.; Jain, R. K.; McDonald, D. M. Openings between Defective Endothelial Cells Explain Tumor Vessel Leakiness. *Am. J. Pathol.* **2000,** *156*, 1363–1380.
8. Dickerson, E. B.; Dreaden, E. C.; Huang, X.; El-Sayed, I. H.; Chu, H.; Pushpanketh, S.; McDonald, J. F.; El-Sayed, M. A. Gold Nanorod Assisted Near-Infrared Plasmonic Photothermal Therapy (PPTT) of Squamous Cell Carcinoma in Mice. *Cancer Lett.* **2008,** *269*, 57–66.
9. Macdonald, I. J.; Dougherty, T. J. Basic Principles of Photodynamic Therapy. *J. Porphyrin Phthalocyanine* **2001,** *5*, 105–129.
10. Liao, H.; Hafner, J. H. Gold Nanorod Bioconjugates. *Chem. Mater.* **2005,** *17*, 4636–4641.
11. Vrouenraets, M. B.; Visser, G. W.; Stigter, M.; Oppelaar, H.; Snow, G. B.; van Dongen, G. A. Targeting of Aluminum(III) Phthalocyanine Tetrasulfonate by Use of Internalizing Monoclonal Antibodies: Improved Efficacy in Photodynamic Therapy. *Cancer Res.* **2001,** *61*, 1970–1975.
12. Diamond, K. R.; Farrell, T. J.; Patterson, M. S. Measurement of Fluorophore Concentrations and Fluorescence Quantum Yield in Tissue-Simulating Phantoms Using Three Diffusion Models of Steady-State Spatially Resolved Fluorescence. *Phys. Med. Biol.* **2003,** *48*, 4135–4149.
13. Fernandez, J. M.; Bilgin, M. D.; Grossweiner, L. I. Singlet Oxygen Generation by Photodynamic Agents. *J. Photochem. Photobiol. B* **1997,** *37*, 131–140.
14. Cunderlikova, B.; Gangeskar, L.; Moan, J. Acid−Base Properties of Chlorin e6: Relation to Cellular Uptake. *J. Photochem. Photobiol. B* **1999,** *53*, 81–90.
15. Choi, Y.; McCarthy, J. R.; Weissleder, R.; Tung, C. H. Conjugation of a Photosensitizer to an Oligoarginine-Based Cell-Penetrating Peptide Increases the Efficacy of Photodynamic Therapy. *ChemMedChem* **2006,** *1*, 458–463.
16. Filyasova, A. I.; Kudelina, I. A.; Feofanov, A. V. A Spectroscopic Study of the Interaction of Tetrasulfonated Aluminum Phthalocyanine with Human Serum Albumin. *J. Mol. Struct.* **2001,** *565−566*, 173–176.

17. Moan, J.; Berg, K. The Photodegradation of Porphyrins in Cells Can Be Used To Estimate the Lifetime of Singlet Oxygen. *Photochem. Photobiol.* **1991,** *53*, 549–553.
18. Sharman, W. M.; van Lier, J. E.; Allen, C. M. Targeted Photodynamic Therapy *via* Receptor Mediated Delivery Systems. *Adv. Drug Delivery Rev.* **2004,** *56*, 53–76.
19. Kuo, T. R.; Hovhannisyan, V. A.; Chao, Y. C.; Chao, S. L.; Chiang, S. J.; Lin, S. J.; Dong, C. Y.; Chen, C. C. Multiple Release Kinetics of Targeted Drug from Gold Nanorod Embedded Polyelectrolyte Conjugates Induced by Near-Infrared Laser Irradiation. *J. Am. Chem. Soc.* **2010,** *132*, 14163–14171.
20. Goldberg, S. N.; Gazelle, G. S.; Mueller, P. R. Thermal Ablation Therapy for Focal Malignancy: A Unified Approach to Underlying Principles, Techniques, and Diagnostic Imaging Guidance. *AJR Am. J. Roentgenol.* **2000,** *174*, 323–331.
21. Orendorff, C. J.; Murphy, C. J. Quantitation of Metal Content in the Silver-Assisted Growth of Gold Nanorods. *J. Phys. Chem. B* **2006,** *110*, 3990–3994.
22. Tomayko, M. M.; Reynolds, C. P. Determination of Subcutaneous Tumor Size in Athymic (Nude) Mice. *Cancer Chemother. Pharmacol.* **1989,** *24*, 148–154.